Revista Brasileira de Ciência do Solo

Division – Soil in space and time | Commission – Soil genesis and morphology

Pedogenesis in an Archaeological Dark Earth – Mulatto Earth Catena over Volcanic Rocks in Western Amazonia, Brazil

Luís Antônio Coutrim dos Santos[(1)], Jane Kelly Silva Araujo[(2)], Valdomiro Severino de Souza Júnior[(3)*], Milton César Costa Campos[(4)], Marcelo Metri Corrêa[(5)] and Regilene Angélica da Silva Souza[(6)]

[(1)] Universidade Federal de Santa Maria, Centro de Ciências Rurais, Departamento de Solos, Programa de Pós-Graduação em Ciência do Solo, Santa Maria, Rio Grande do Sul, Brasil.
[(2)] Universidade Federal Rural de Pernambuco, Departamento de Agronomia, Programa de Pós-Graduação em Ciência do Solo, Recife, Pernambuco, Brasil.
[(3)] Universidade Federal Rural de Pernambuco, Departamento de Agronomia, Recife, Pernambuco, Brasil.
[(4)] Universidade Federal do Amazonas, Instituto de Educação, Agricultura e Meio Ambiente, Departamento de Agronomia, Humaitá, Amazonas, Brasil.
[(5)] Universidade Federal Rural de Pernambuco, Unidade Acadêmica de Garanhuns, Departamento de Agronomia, Garanhuns, Pernambuco, Brasil.
[(6)] Universidade Federal Rural da Amazônia, Instituto de Ciências Agrárias, Departamento de Agronomia, Belém, Pará, Brasil.

ABSTRACT: Archaeological Dark Earth (ADE) pedogenesis and pre-Columbian history are fundamental for understanding the biodiversity and pedodiversity of the Neotropical rainforest in the Amazon region. This study aimed to evaluate the morphological, physical, chemical, and mineralogical properties as well as NaOH-extractable organic matter [OM(NaOH)] in ADE and Mulatto Earth (ME) overlying volcanic rocks along a toposequence (four soil profiles) in western Amazonia, Brazil. The soil profiles show anthropic A horizons over an argic horizon (Bt) in the ADE (Humic, Pretic Luvisols) and Bi in the ME (Clayic, Dystric Cambisols). The soil-forming processes in all of the profiles are associated with organic matter accumulation, such as humification and melanization, besides the formation of organometallic complexes. Calcium, Mg, P, and organic carbon contents were higher in ADE compared to ME. High-activity clays are derived from parent volcanic material, distinguishing the soils studied from Amazonian soils (Tertiary Plateau, *Terra Firme*) and most Amazonian anthropic soils. The anthropic horizons generally have a large contribution from OM(NaOH), predominantly humin and humic acids associated with Ca, Mg, and poorly crystalline Al hydroxides. The results suggest that the anthropic driving-forces caused greater differences in pedogenesis than the soil location in the landscape.

Keywords: Amazonian soils, anthropogenesis, pretic horizon, humin, Luvisols.

*** Corresponding author:**
E-mail: valdomiro.souzajunior@ufrpe.br

Received: November 6, 2017
Approved: April 3, 2018

How to cite: Santos LAC, Araujo JKS, Souza Júnior VS, Campos MCC, Corrêa MM, Souza RAS. Pedogenesis in an Archaeological Dark Earth – Mulatto Earth catena over volcanic rocks in western Amazonia, Brazil. Rev Bras Cienc Solo. 2018;42:e0170359.
https://doi.org/10.1590/18069657rbcs20170359

INTRODUCTION

Archaeological Dark Earth (ADE), also known as *Terra Preta de Índio*, contrasts with non-anthropogenic soils of the Amazonas region due to the high content of organic matter and carbon in the highly stable form of biochar (pyrogenic carbon), and usually these soils are rich in P and Ca. Pedogenesis of ADE and the role of pre-Columbian nations form one of the most important and complex archaeological data sources for understanding the pedodiversity, Amazonian prehistory, and the anthropic driving forces in the soil environment. The anthropogenesis is complex and wide ranging on the spatio-temporal scale, encompassing many processes and outcomes (Sandor et al., 2005). Such anthropogenic processes are important to support the pedology (Bryant and Galbraith, 2003) and the sustainability of agricultural areas of the anthropic soils, which range from black and brownish (*Terra Mulata* or Mulatto Earth – ME) coloration.

The ME is another soil type in the Amazon whose formation is related to long-term indigenous crops (Sombroek, 1966; Arroyo-Kalin, 2012; Costa et al., 2013; Roberts et al., 2017). The MEs are pre-Colombian farming areas near the ADEs, stemming from improved soil fertility due to agriculture, likely using practices similar to composting (Sombroek et al., 2009). The ME areas are distinguished from the ADE by their lighter-colored surface layer and the absence or small number of ceramic artifacts, which are frequently near the different ADE sites (Sombroek et al., 2009). This soil type is controverted and is rarely reported in the literature, in addition to having poor nutrient content compared to ADE. However, ME has higher levels of exchangeable bases compared to the adjacent Ferralsols and Ultisols, with slight increases in pH and P, Ca, Mg, Mn, and Zn contents (Fraser et al., 2011).

Archaeological Dark Earth has anthropogenic A horizons and is classified as Pretic Anthrosol by the IUSS Working Group WRB (2015). The pretic horizon is defined as a dark mineral surface horizon with a Munsell color value ≤4 and a chroma ≤3, both moist, a soil organic carbon content of ≥10 g kg^{-1}, an exchangeable Ca plus Mg content ≥2 $cmol_c$ kg^{-1}, and Mehlich-1 extractable P ≥30 mg kg^{-1}. In addition, it contains ≥1 % artifacts (by volume), or charcoal content ≥1 % (by volume), or evidences of past human occupation in the surrounding landscape, e.g., constructions, gardens, shell mounds, or earthworks; and <25 % (by volume, by weighted average) of animal pores, coprolites, or other traces of soil animal activity; and one or more layers with a combined thickness of ≥0.20 m. The pretic horizons are the result of pre-Columbian activities and have persisted over many centuries despite humid tropical conditions (IUSS Working Group WRB, 2015).

These soils occur in patches throughout the Amazon, particularly in Brazil, Colombia, Guyana, Ecuador, Peru, and Venezuela (Kern et al., 2003). These areas are located over ancient settlements where several cultural artifacts are found. Their dark color is due to organic matter decomposition in the form of pyrogenic carbon (biochar, charcoal), such as domestic fire and agricultural burning remnants (Lima et al., 2002). The NaOH-extractable organic matter [OM(NaOH)] has a high amount of inorganic impurities (Ca, Fe, Al, and Si) (Swift, 1996). The humin fraction may be composed of organic matter that is strongly bound to the mineral phase (Sollins et al., 1996), which may include charcoal and condensed polyaromatic structures (Knicker et al., 2005; Schellekens et al., 2017), with a relatively low degree of degradation of organic matter in anthropogenic horizons (Glaser et al., 2003; Schellekens et al., 2017).

The ADEs are recurring over various soil classes, especially Ferralsols, Acrisols, and Cambisols (Lima et al., 2002), as well as Leptosols/Regosols (Santos et al., 2013a) and Podzols (Smith, 1980). However, the occurrence of ADE on Luvisols had not yet been reported for the Amazon region.

It is believed that humans and many other organisms, which are active agents of soil formation, have interacted with the Earth's surface and changed the soil composition during its genesis (Sandor et al., 2005). Anthropogenic soils are the result of different

uses and durations of indigenous settlements in distinct patterns of soil modification, which indicate the location of functional areas of villages, due to the distinct properties of their occupation (Lima et al., 2002; Lehmann et al., 2003; Arroyo-Kalin et al., 2009; Arroyo-Kalin, 2012). While soils are subjected to major changes over geological time, changes due to anthropogenic activity commonly occur over a much shorter time scale (Sandor et al., 2005). Anthropogenic activity can promote argilluviation and the development of clay coating (Macedo et al., 2017).

Furthermore, other studies have investigated relationships between soil properties and landscape at different locations. Anthropogenic A horizons with similar chemical properties and depths in different relief positions were observed by Campos et al. (2011), suggesting that similar anthropogenic conditions have influenced their formation. Although substantial information is available on ADEs (Kern and Kämpf, 1989; Costa and Kern, 1999; Lima et al., 2002; Campos et al., 2012; Santos et al., 2013a; Macedo et al., 2017), the origin of such soils remains a challenge, as well as optimization of their use and management. There is thus a large knowledge gap in relative to the anthropic driving-forces expressed in the ADE and ME, especially related to landscape locations and derivation from intermediate volcanic rocks. The common parent material of *Terras Firmes* are granites and tertiary sediments (Brasil, 1978), which are reflected, to a certain extent, in the mineralogical composition of the soils (low activity clay) and the poverty of mafic minerals of the parent material, associated with intense chemical weathering, typical of the Amazon region.

We hypothesize that the anthropic soils of Apuí, Amazonas state, have different properties than other soils of the Amazon region because they are developed on volcanic rocks. Furthermore, differences in the composition of soil organic matter between ADE and ME affect the accumulation of carbon in these soils. Consequently, we aimed to evaluate soil pedogenesis along a toposequence from Archaeological Dark Earth to Mulatto Earth, overlying volcanic rocks in the western Amazon, Brazil.

MATERIALS AND METHODS

The soil toposequence studied is in the western Amazon, in the south-central part of the state of Amazonas (Brazil), municipality of Apuí (Figure 1). The location of the soil profiles and current use of the soil are as follows: P1 (summit, 7° 12’ 00” S, 59° 39’ 35” W, old forest); P2 (shoulder, 7° 12’ 3’’ S, 59° 39’ 35” W, cacao plantation); P3 (backslope, 7° 12’ 8” S, 59° 39’ 35” W, brachiaria/kudzu); and P4 (footslope, 7° 12’ 9” S, 59° 39’ 36” W, brachiaria/kudzu). The climate is hot and humid with a brief dry season and “Am” type (monsoon-type rain) by the Köppen classification system. Average annual temperature ranges from 25 to 26 °C, with annual rainfall ranging from 1,750 to 2,750 mm, a short dry period with less than 60 mm of rainfall in the dry months, and relative humidity of 85 % (Brasil, 1975).

The area has no major elevation and is composed of lowlands and hilly areas, as well as regular and highland plateaus, which can reach 400 m altitude. The toposequence was identified from the summit to the footslope, with alluvial sediments from the Douradão River. The toposequence was subdivided into four segments based on the model of Dalrymple et al. (1968). The profiles P1, P2, P3, and P4 are at 117, 113, 96, and 93 m a.s.l., respectively (Figure 2). Vegetation in the area is primarily dense forests (Brasil, 1975).

Local geology is defined by the Colider Group, which is composed of rhyolites, rhyodacites, basalts, andesites, tuffs, volcanic breccias, and interspersed epiclastic beds (CPRM, 2005).

A pit was dug in each slope segment for further soil morphological characterization and sampling. The soil samples were used for physical and chemical analyses. Soil horizons were identified and the morphology was described according to Santos et al. (2015). Ceramic fragments in the soil samples were quantified by weighing, establishing the

ratio [mass of ceramic fragments/mass of the air-dried fine earth (ADFE)]. The soils were classified according to the Brazilian System of Soil Classification (SiBCS) (Santos et al., 2013b) and the World Reference Base of Soils (IUSS Working Group WRB, 2015). Rock samples with signs of alteration were also collected from the base of the P1 and P3 profiles. The rock samples were fragmented and reduced for mineralogical analyses.

Particle size distribution analysis was performed after removal of organic matter with hydrogen peroxide (H_2O_2). The clay fraction was measured with a hydrometer after dispersion with an NaOH solution at 0.01 mol L^{-1}. The coarse and fine sand fractions were separated through sieving, and then dried and weighed. The silt fraction was calculated based on the difference between the total sand weight and the clay weight, according to Gee and Or (2002). Water dispersed clay (WDC) was determined by the densimeter method, and the degree of flocculation (DF) was calculated (Donagema et al., 2011).

Soil bulk density (Bd) was determined using the volumetric ring method as proposed by Grossman and Reinsch (2002). The soil solid particle density (ρs) was determined using the volumetric flask method as proposed by Flint and Flint (2002). Total soil porosity (Pt) was estimated from the particle and soil densities using the following expression: Pt = 100 × (1- Bd/ρs) (Donagema et al., 2011).

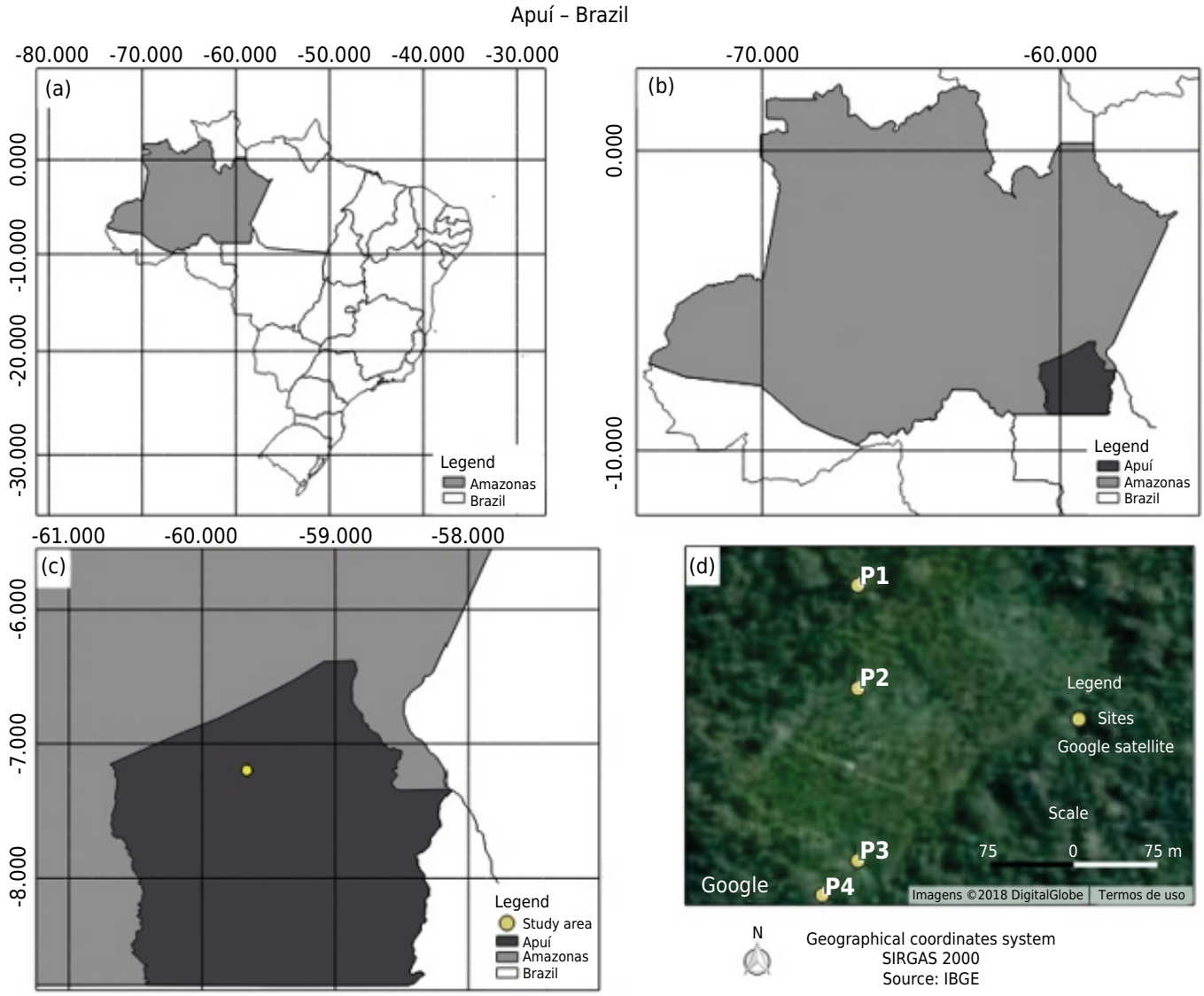

Figure 1. Location of the studied area in western Amazonia, Brazil.

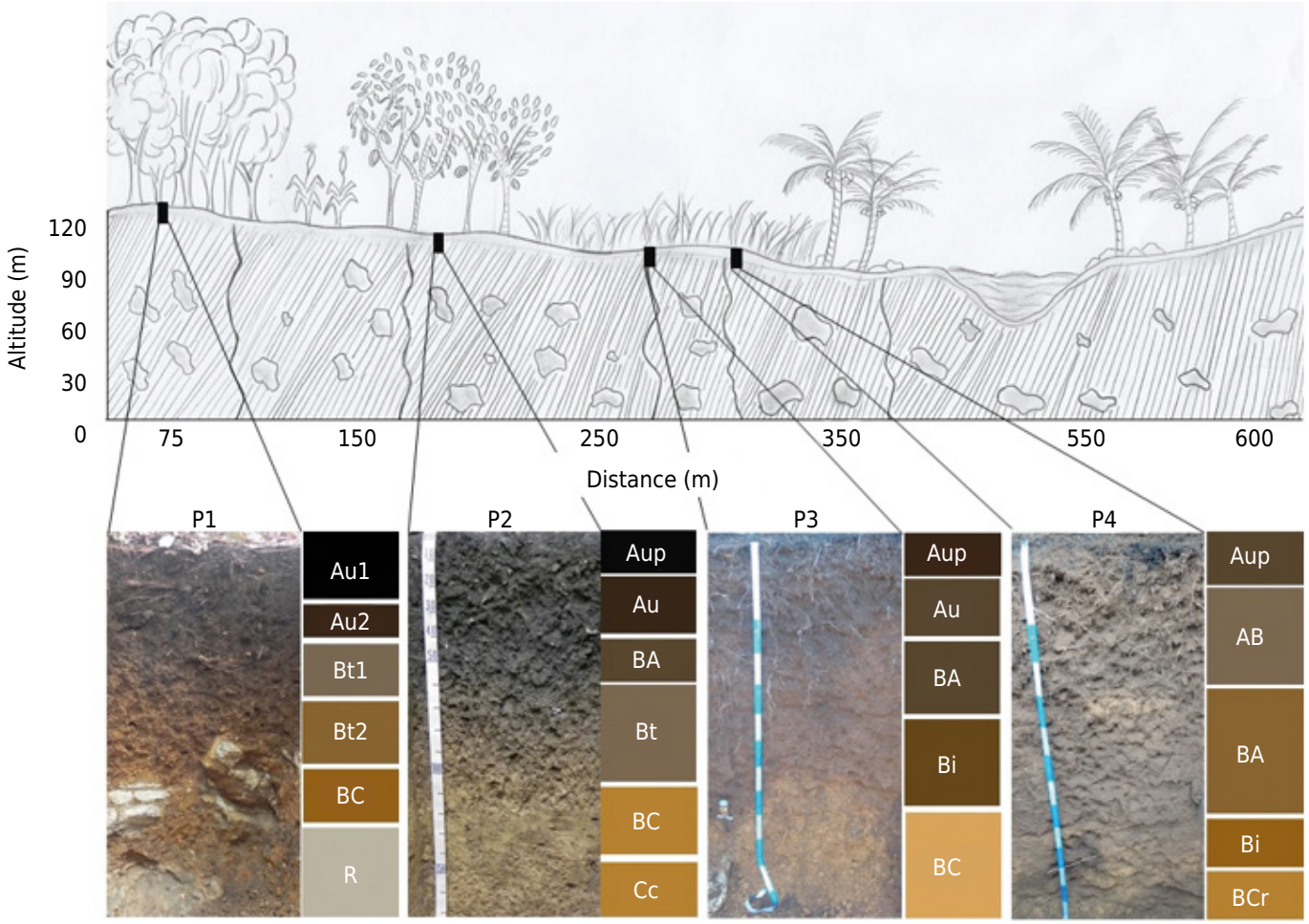

Figure 2. Location of the four profiles of the volcanic toposequence studied in Apuí (Brazil).

Soil pH was measured in water and in a KCl 1 mol L^{-1} solution using a potentiometer and a ratio of 1:2.5 v/v of soil:liquid. Exchangeable Ca, Mg, and Al were extracted with KCl 1 mol L^{-1} and determined using atomic absorption spectrophotometry. Exchangeable K, Na, and available P were extracted with Mehlich-1. Concentrations of K^+ and Na^+ were determined through flame spectrophotometry, and available P through colorimetry. Potential acidity (H+Al) was extracted using 0.5 mol L^{-1} calcium acetate solution buffered at pH 7.0, which was determined by titration with 0.025 mol L^{-1} NaOH. Based on chemical analyses, we calculated the sum of bases (SB), cation exchange capacity (CEC), base saturation (V), and aluminum saturation (m). All the chemical analyses mentioned above were determined according to Donagema et al. (2011).

Clay fraction mineralogy was studied using X-ray diffraction (XRD), after a pretreatment to remove organic matter using 3 % H_2O_2 (v/v) (Jackson, 1975). Chemical dispersion of the particle size fractions was performed with NaOH and plus mechanical agitation with a "Wagner" for 16 h. The clay fraction was separated by siphoning after decantation of the silt fraction. Diffractograms were produced from samples in the form of natural oriented clay. The criterion used to interpret the diffractograms and identify the minerals was based on interplanar spacing (d), according to Jackson (1975) and Brown and Brindley (1980).

Silicon, Fe, and Al were extracted by sulfuric acid digestion, followed by alkaline digestion. These elements were determined in the upper, middle, and lower horizons of each soil profile using the fine earth fraction, based on the methodology proposed by Vettori (1969). Measurements were recorded using atomic absorption spectrophotometry.

Free Fe (Fed) was extracted using dithionite-citrate-bicarbonate (DCB) with three successive extractions for 15 min at 80 °C, as described by Mehra and Jackson (1960) with modifications of Inda Junior and Kämpf (2003). The low-crystallinity Fe (Feo) and Al (Alo) forms were extracted using a 0.2 mol L^{-1} ammonium oxalate solution at a pH of 3.0 in the dark for a single extraction (Schwertmann, 1964). The amounts were measured through atomic absorption spectrophotometry. The Fed and Feo were expressed in g kg^{-1}, and the following ratios were determined: Feo/Fed and Feo/(Fed-Feo). Moreover, Fe contents were converted to the oxide form (Fe_2O_3) to determine the ratio between the DCB extracted Fe contents and those extracted via sulfuric acid attack, Fed/Fes.

Total organic carbon (TOC) was determined via wet oxidation with external heating using a 0.167 mol L^{-1} potassium dichromate solution and concentrated sulfuric acid (Yeomans and Bremner, 1988). The separation of OM(NaOH) was performed according to Mendonça and Matos (2005) using 0.5 g of soil in 10 mL of 0.1 mol L^{-1} NaOH for 16 h in an automatic shaker at a soil:extractant ratio of 1:20. The extractable material and the final residue are similar to the operationally defined humic acid (HA), fulvic acid (FA), and humin (HUM) fractions (Lichtfouse et al., 1998). The TOC contents in each fraction (HA, FA, and HUM) were analyzed according to Yeomans and Bremner (1988).

The relationship between carbon content in the form of humic acids (C-HA) and fulvic acids (C-FA) were used to indicate carbon mobility (Benites et al., 2003) or the potential of soil carbon loss (Anjos et al., 2008). The ratio of the alkaline extract carbon content (sum of C-FA and C-HA) and the humin fraction carbon content (C-HUM) was used to indicate the structural stability of organic matter.

The soil variables and soil organic matter (SOM) fractions of all the horizons were analyzed through Pearson correlations. Analyses were performed using the statistical program Statistica 12.0 (Statsoft Inc., 2013).

RESULTS

Morphological and physical properties

Diagnostic horizons in each pedon include anthropic A horizons (Au) overlying a diagnostic argic subsurface horizon (Bt horizons) in the ADE (P1 and P2) and Bi in the ME (P3 and P4). The pedons exhibit Au1-Au2-Bt1-Bt2-BC-R (P1), Aup-Au-BA-Bt-BC-Cc (P2), Aup-Au-BA-Bi-BCr (P3), and Aup-AB-BA-Bi-BCr (P4) pedogenic horizon sequences (Table 1). Darker colors in the surface horizons of the P1 and P2 profiles range from black to very dark brown (moist color) (0.00-0.33 m in P1 and 0.00-0.45 m in P2), associated with the greater occurrence of ceramic fragments incorporated in these horizons (Tables 1). For the P3 and P4 profiles, the surface horizons (depth <0.24 m in P3 and depth <0.49 m in P4) range from very dark brown to very dark grayish brown.

The subsurface horizons of the ADE have moderate to abundant occurrences of clay coatings in the soil aggregates, inter- and intra-aggregates, defined as the Bt horizon, although the clay content is insufficient to characterize the textural gradient. The silt and clay fractions are predominant, and the clay fraction tends to increase with depth from the anthropic horizon to the subsurface horizon in the ADE. The silt fraction, however, behaves differently. The horizons of the ADE range from silty clay loam to silty clay, while the ME texture is clayey in all horizons (Table 2). The silt/clay ratio in the profiles studied has higher values in the anthropic horizon than in the subsurface horizon, primarily for the P1 and P2 profiles. The anthropic horizons of all the soils have a strong and/or moderate structure in granular and/or block forms (Table 1).

The degree of flocculation of clay increases at the surface (Table 2). Bulk densities are lowest in the upper horizons (Table 2). The mean ρs has approximately the same values (2.6 Mg m^{-3}) throughout the entire toposequence.

Table 1. Morphological properties of Archaeological Dark Earth and Mulatto Earth in western Amazonia, Brazil

Horizon	Layer	Ceramic fragments	Color (wet)	Clay coating	Structure
	m				
P1 - Summit - Humic, Pretic Luvisol/*Luvissolo Crômico* (Archaeological Dark Earth)					
Au1	0.00-0.20	67	10YR 2/1	nc	str. sma. to med. gra.
Au2	0.20-0.33	31	10YR 2/2	nc	mod. sma. to med. gra. and sub
Bt1	0.33-0.50	8	10YR 4/3	nc	mod. vsma. med. and sub
Bt2	0.50-0.68	0	10YR 4/4	mod. and com.	wea. and mod. med. angb
BC	0.68-0.83	0	10YR 4/6	wea. and com.	wea. med. angb
R	0.83-1.37+	0	nd	nd	nd
P2 - Shoulder - Humic, Pretic Luvisol/*Luvissolo Crômico* (Archaeological Dark Earth)					
Aup	0.00-0.16	54	10YR 2/1	nc	mod. and str. vsma. and sma. gra. and sub
Au	0.16-0.45	33	10YR 2/2	nc	mod. and str. vsma. sma. gra.
BA	0.45-0.62	0	10YR 3/3	nc	mod. vsma. and sma. sub
Bt	0.62-1.05	0	10YR 4/3	mod. and abu.	wea. med. angb
BC	1.05-1.35	0	10YR 5/6	nc	ma.
Cc	1.35-1.80+	0	10YR 5/6	nc	nd
P3 - Backslope - Clayic, Dystric Cambisol/*Cambissolo Háplico* (Mulatto Earth)					
Aup	0.00-0.11	0	10YR 2/2	nc	str. vsma. sma. gra.
Au	0.11-0.24	12	10YR 3/1	nc	mod. med. to lar. angb subb and gra.
BA	0.24-0.50	0	10YR 3/2	nc	str. sma. and med. angb subb and gra.
Bi	0.50-0.85	0	10YR 3/3	nc	str. lar. to vlg. angb and sub
BCr	0.85-1.10+	0	10YR 6/6	nc	ma.
P4 - Footslope - Clayic, Dystric Cambisol/*Cambissolo Háplico* (Mulatto Earth)					
Aup	0.00-0.23	3	10YR 3/2	nc	str. sma. gra.
AB	0.23-0.49	0	10YR 4/3	nc	mod. med. angb
BA	0.49-0.92	0	10YR 4/4	nc	str. med. to lar. angb
Bi	0.92-1.27	0	10YR 4/6	nc	str. med. to lar. gra.
BCr	1.27-1.40+	0	10YR 5/6	nc	ma.

abu = abundant; angb = angular blocks; com = common; gra = granular; lar = large; med = medium; mod = moderate; ma = massive; nc = unchecked; nd = non-determined; sma = small; str = strong; sub = subangular blocks; vlg = very large; vsma = very small; wea = weak.

Chemical properties and extractions of Si, Fe, and Al

The total organic carbon (TOC) content of the bulk samples decreases throughout the toposequence (Table 3). In the uppermost horizon, TOC ranges from 56.3 to 68.8 g kg^{-1} in the ADE and from 37.6 to 49.5 g kg^{-1} in the ME.

The Ca^{2+} contents range from 2.39 to 23.85 $cmol_c$ kg^{-1}, and the Mg^{2+} from 0.13 to 4.14 $cmol_c$ kg^{-1}, in the anthropic horizons, while P4 has the lowest values in this horizon (from 1.84 to 10.59 $cmol_c$ kg^{-1} for Ca^{2+} and from 0.05 to 0.43 $cmol_c$ kg^{-1} for Mg^{2+}) (Table 3). These results are similar to those determined by Silva et al. (2011), who reported Ca^{2+} contents from 3.20 to 25.0 $cmol_c$ kg^{-1}. The K^+ contents are low, ranging from 1.44 to 0.02 $cmol_c$ kg^{-1} in all horizons (Table 3). The P3 profile has the highest K^+ content.

The pH(KCl) is lower than the pH(H_2O), establishing a negative ΔpH (Table 3), with values higher than 5.5 in the ADE, and from 4.4 to 6.0 in the ME. The CEC values are high in all the profiles, primarily in the Au and Aup horizons. The highest V percentages are observed in the ADE, including the subsurface horizons, classified as eutrophic, whereas the ME are dystrophic, with the exception of the Aup horizon of the P3 profile. The available P contents are high, at an average of 290 mg kg^{-1} in the surface horizons. The P2 Au horizon stands out with 662 mg kg^{-1}, whereas the P4 profile has the lowest values (162 mg kg^{-1} in the anthropic horizon).

Sulfuric acid digestion results in the highest contents of Si, Fe, and Al oxides in the ADE profiles, except for the Aup of P4, which shows higher value of SiO_2 (Table 4). The values of total Fe_2O_3 and Fed are higher in the ADE profiles than in the ME profiles. The total Fe_2O_3 contents range from 32.3 to 98.8 g kg^{-1} (Table 4), within the typical range of values observed in Amazonian soils (Silva et al., 2011). The Fed contents range from 32.2 to 61.9 g kg^{-1} (ADE) and from 8.7 to 27.2 g kg^{-1} (ME), which predominates over the forms of Feo.

The Fed/Fes ratio has been used as an indicator of the degree of soil development, with higher values in weathered soils (Cunha et al., 2005). The highest values of the ratio are observed in the ADE profiles, confirming the more advanced evolution of these soils compared to the rest of the toposequence. The Feo/Fed ratio is low for all soils studied throughout the toposequence. Additionally, the Feo/(Fed-Feo) ratio, in which the Feo contents are subtracted from Fed, is low in the ADEs and high in the MEs. The higher Feo/(Fed-Feo) ratios presented for MEs indicate a dominance of low-crystallinity Fe-forms and confirm the incipient nature of these soils (Lima et al., 2002), classified as *Cambissolo*.

The Ald contents has the highest values for P1 (ranging from 27.59 to 30.03 g kg^{-1}) and these contents decrease along the toposequence. The lowest values are observed for P3 and P4 (7.42 to 11.53 g kg^{-1}). No significant variation of these values is observed

Table 2. Physical properties of Archaeological Dark Earth and Mulatto Earth in western Amazonia, Brazil

Horizon	FS/CS	Particle size distribution[(1)]				WDC	DF	Silt/Clay	Bd	Ps	Pt
		Coarse sand	Fine sand	Silt	Clay						
		g kg^{-1}					%		Mg m^{-3}		m^3 m^{-3}
P1 - Summit - Humic, Pretic Luvisol/*Luvissolo Crômico* (Archaeological Dark Earth)											
Au1	1.4	65	93	451	391	43	89	1.2	0.7	2.5	72
Au2	1.4	63	88	443	406	180	56	1.1	0.9	2.6	65
Bt1	1.5	43	67	336	554	277	50	0.6	nd	2.7	nd
Bt2	1.4	27	38	332	603	348	42	0.6	nd	2.7	nd
BC	1.4	23	32	217	728	455	38	0.3	nd	2.7	nd
P2 - Shoulder - Humic, Pretic Luvisol/*Luvissolo Crômico* (Archaeological Dark Earth)											
Aup	1.5	62	91	454	393	109	72	1.2	0.9	2.6	65
Au	1.6	58	92	446	404	269	33	1.1	0.9	2.6	65
BA	1.9	35	65	334	566	362	36	0.6	1.2	2.7	56
Bt	1.5	23	34	330	613	454	26	0.5	nd	2.7	nd
BC	2.1	16	33	250	701	467	33	0.4	nd	2.7	nd
Cc	0.9	35	33	213	719	479	33	0.3	nd	nd	nd
P3 - Backslope - Clayic, Dystric Cambisol/*Cambissolo Háplico* (Mulatto Earth)											
Aup	1.1	84	100	380	436	138	68	0.9	0.8	2.5	69
Au	1.3	85	112	289	514	187	64	0.6	0.9	2.6	65
BA	1.6	68	107	265	560	234	58	0.5	1.0	2.7	63
Bi	2.0	56	110	263	571	286	50	0.5	1.1	2.7	61
BCr	2.2	36	81	312	571	119	79	0.5	nd	2.7	nd
P4 - Footslope - Clayic, Dystric Cambisol/*Cambissolo Háplico* (Mulatto Earth)											
Aup	1.8	51	92	352	505	229	55	0.7	0.8	2.5	69
AB	2.5	40	99	352	509	255	50	0.7	0.8	2.6	69
BA	2.4	41	100	353	506	184	64	0.7	1.0	2.7	64
Bi	2.2	46	103	331	520	331	36	0.6	1.2	2.7	55
BCr	2.3	46	104	328	522	285	45	0.6	nd	2.7	nd

[(1)] Sand, silt, clay: method described in Gee and Or (2002); WDC: water-dispersed clay (Donagema et al., 2011); DF: degree of flocculation (Donagema et al., 2011); FS/CS = fine sand/coarse sand ratio; Bd = soil bulk density (Grossman and Reinsch (2002); Ps = particle density (Flint and Flint, 2002); Pt = total porosity, calculated according to Donagema et al. (2011); nd = not determined.

Table 3. Chemical properties of Archaeological Dark Earth and Mulatto Earth in western Amazonia, Brazil

Profile	Hz	pH		ΔpH	Ca^{2+}	Mg^{2+}	K^{+}	Na^{+}	SB	Al^{3+}	H+Al	CEC	V	m	P	TOC	CECa
		H_2O	KCl														
					cmol$_c$ kg^{-1}								%		mg kg^{-1}	g kg^{-1}	
P1 - Summit - Humic, Pretic Luvisol/*Luvissolo Crômico* (Archaeological Dark Earth)																	
P1	Au1	5.50	5.00	-0.5	23.85	4.14	0.19	0.08	28.26	0.58	15.49	43.75	65	2	206	68.85	111.89
	Au2	5.70	4.70	-1.0	14.64	2.27	0.09	0.05	17.05	0.43	14.27	31.32	54	2	455	37.23	77.14
	Bt1	5.90	4.70	-1.2	12.07	2.07	0.09	0.06	14.29	0.42	8.84	23.13	62	3	268	20.87	41.75
	Bt2	5.80	4.50	-1.3	8.90	1.20	0.09	0.05	10.24	0.38	6.76	17.00	60	4	128	10.61	28.19
	BC	5.70	4.50	-1.2	7.42	0.69	0.14	0.05	8.30	0.40	6.26	14.56	57	5	146	7.29	20.00
P2 - Shoulder - Humic, Pretic Luvisol/*Luvissolo Crômico* (Archaeological Dark Earth)																	
P2	Aup	6.30	5.70	-0.6	21.60	1.87	0.52	0.10	24.09	0.78	8.50	32.59	74	3	227	56.31	82.93
	Au	5.80	4.60	-1.2	13.89	2.22	0.43	0.11	16.65	0.38	16.81	33.46	50	2	668	32.75	82.82
	BA	5.80	4.50	-1.3	10.82	1.99	0.21	0.07	13.09	0.42	12.48	25.57	51	3	354	16.60	45.18
	Bt	5.60	4.40	-1.2	8.29	1.33	0.17	0.07	9.86	0.49	7.72	17.58	56	5	203	9.55	28.68
	BC	5.40	4.30	-1.1	6.58	1.33	0.16	0.06	8.13	0.55	6.62	14.75	55	6	199	5.62	21.04
	Cc	5.20	4.20	-1.0	5.00	1.30	0.14	0.06	6.50	0.52	6.20	12.70	51	7	226	4.89	17.66
P3 - Backslope - Clayic, Dystric Cambisol/*Cambissolo Háplico* (Mulatto Earth)																	
P3	Aup	6.00	5.40	-0.6	18.52	2.88	0.50	0.15	22.04	0.03	11.60	33.64	66	0	236	49.50	77.16
	Au	5.60	4.10	-1.5	2.39	0.13	1.44	0.29	4.25	1.55	20.39	24.65	17	27	323	26.33	47.96
	BA	5.50	4.00	-1.5	1.52	0.02	1.42	0.15	3.11	1.79	15.98	19.09	16	37	284	13.72	34.09
	Bi	4.80	3.90	-1.0	1.49	0.01	0.53	0.08	2.11	2.17	13.69	15.80	13	51	258	9.95	27.67
	BCr	4.60	3.60	-1.0	1.53	0.01	0.22	0.03	1.79	2.84	10.31	12.10	15	61	140	4.61	21.19
P4 - Footslope - Clayic, Dystric Cambisol/*Cambissolo Háplico* (Mulatto Earth)																	
P4	Aup	5.00	4.20	-0.8	10.59	0.43	0.27	0.17	11.47	0.57	19.87	31.34	37	5	162	37.60	62.06
	AB	4.40	4.00	-0.5	1.84	0.05	0.09	0.13	2.11	2.45	17.20	19.31	11	54	119	22.70	37.94
	BA	4.70	4.00	-0.7	1.74	0.01	0.04	0.00	1.80	2.20	13.62	15.41	12	55	107	9.70	30.45
	Bi	4.50	3.90	-0.6	1.70	0.00	0.02	0.00	1.73	2.62	9.87	11.59	15	60	73	3.99	22.29
	BCr	4.50	4.00	-0.5	1.57	0.01	0.02	0.00	1.59	2.51	10.52	12.11	13	61	95	6.02	23.20

Hz = horizon; SB = sum of bases; CEC = cation exchange capacity; V = base saturation; m = aluminum saturation, all calculate according to Donagema et al. (2011); TOC = total organic carbon (Yeomans and Bremner, 1988); CECa = clay fraction activity (Donagema et al., 2011).

throughout each profile. The Alo values are lower than the Ald values and have a similar variation with higher values for P1 (mean of 11.8 g kg^{-1}) (Table 4). The TiO_2 contents show small variation with depth and between anthropogenic soils.

Mineralogical properties

Kaolinite is the predominant mineral in the clay fraction for all the anthropogenic soils evaluated, which is identified by the presence of diffraction peaks relative to the basal spacing at 0.357 and 0.716 nm. In general, gibbsite, goethite, mica, and feldspars are also found in the clay fraction of all the profiles studied (Figure 3). Gibbsite is identified by diffraction peaks at 0.484 nm, goethite by peaks at 0.415 nm, mica by peaks at 1.00 nm, and feldspars by peaks at 0.335 nm. Traces of expansive minerals (diffraction peaks from 1.23-1.36 nm) are observed in most profiles, with higher values in P4 and absence in P2 (Figure 3). The P1 and P3 profile rocks have mineralogical compositions similar to the soil clay fraction, such as kaolinite, feldspar, quartz, gibbsite, and biotite (Figure 3). The presence of kaolinite and gibbsite is indicative of alteration.

Contribution of OM(NaOH) to the formation of the anthropic A horizon

The anthropic horizons contain a large contribution of extractable OM(NaOH), primarily HUM and HA (Table 4). The C-HUM ranges from 12.49 to 37.30 g kg^{-1} in the anthropic horizons, with a decreasing humin fraction with depth in all the profiles studied, corresponding, on average, to 55 % of TOC in all the profiles. In P2, this proportion tends to be slightly higher, reaching up to 71 % of TOC in Aup. The C contents in the humic acid (C-HA) extracts decrease with depth, ranging from 10.5 to 14.5 g kg^{-1} in the anthropic horizons.

Table 4. Extractions of silicon, iron, aluminum, titanium, and fractions of the NaOH-extractable organic matter of Archaeological Dark Earth and Mulatto Earth in western Amazonia, Brazil

Horizon	SiO_2	Al_2O_3	Fe_2O_3	TiO_2	Ki	Fed	Feo	Ald	Alo	Feo/Fed	Feo/(Fed-Feo)	Fed/Fes	C-FA	C-HA	C-HUM	C-HA/C-FA	C-AE/C-HUM
	g kg^{-1}					g kg^{-1}							g kg^{-1}				
P1 – Summit – Humic, Pretic Luvisol/*Luvissolo Crômico* (Archaeological Dark Earth)																	
Au1	166.0	161.8	76.9	8.60	1.74	47.57	5.41	29.95	13.98	0.11	0.13	0.62	4.17	17.48	35.67	4.20	0.61
Au2	nd	nd	nd	nd	nd	41.38	5.37	30.03	9.94	0.13	0.15	nd	2.26	12.77	17.05	5.64	0.88
Bt1	nd	nd	nd	nd	nd	45.75	6.46	27.59	3.89	0.14	0.16	nd	0.91	4.89	10.99	5.40	0.53
Bt2	239.0	225.6	90.9	7.90	1.80	54.26	4.01	28.59	2.27	0.07	0.08	0.60	0.81	0.45	8.94	0.56	0.14
BC	244.0	239.7	98.4	6.90	1.73	53.74	3.80	29.27	2.47	0.07	0.08	0.55	0.81	0.18	6.73	0.22	0.15
P2 – Shoulder – Humic, Pretic Luvisol/*Luvissolo Crômico* (Archaeological Dark Earth)																	
Aup	155.5	152.0	62.7	8.10	1.74	32.18	4.55	23.27	8.50	0.14	0.16	0.51	2.99	11.95	37.30	4.00	0.40
Au	nd	nd	nd	nd	nd	36.96	4.80	24.85	8.14	0.13	0.15	nd	2.17	14.49	15.13	6.67	1.10
BA	nd	nd	nd	nd	nd	37.21	3.44	25.77	2.54	0.09	0.10	nd	1.81	4.35	10.78	2.40	0.57
Bt	266.0	237.8	86.5	7.70	1.90	45.85	4.12	23.99	2.22	0.09	0.10	0.53	0.36	1.09	7.68	3.00	0.19
BC	nd	nd	nd	nd	nd	46.02	3.16	22.80	2.12	0.07	0.07	nd	0.18	0.45	6.50	2.50	0.10
Cc	285.0	262.3	98.8	7.30	1.85	61.92	2.39	24.67	2.09	0.04	0.04	0.63	0.81	0.54	5.51	0.67	0.25
P3 – Backslope – Clayic, Dystric Cambisol/*Cambissolo Háplico* (Mulatto Earth)																	
Aup	133.5	122.4	57.5	7.30	1.85	9.39	4.02	9.23	7.54	0.43	0.75	0.16	6.88	13.40	34.88	1.95	0.58
Au	nd	nd	nd	nd	nd	11.21	4.29	10.30	7.96	0.38	0.62	nd	4.26	13.40	12.49	3.15	1.41
BA	nd	nd	nd	nd	nd	14.28	4.25	9.58	6.06	0.30	0.42	nd	2.26	5.43	6.13	2.40	1.26
Bi	150.5	161.9	59.5	8.40	1.58	11.18	3.56	8.69	4.81	0.32	0.47	0.19	2.72	3.71	4.88	1.37	1.32
BCr	231.0	201.9	67.7	9.30	1.94	8.73	1.51	7.42	2.35	0.17	0.21	0.13	2.17	0.18	6.08	0.08	0.39
P4 – Footslope – Clayic, Dystric Cambisol/*Cambissolo Háplico* (Mulatto Earth)																	
Aup	187.5	132.5	32.3	9.40	2.41	13.21	6.10	9.25	4.38	0.46	0.86	0.41	7.24	10.49	26.33	1.45	0.67
AB	nd	nd	nd	nd	nd	24.43	5.15	11.46	4.71	0.21	0.27	nd	4.98	5.56	10.59	1.12	1.00
BA	nd	nd	nd	nd	nd	25.16	4.75	11.53	4.38	0.19	0.23	nd	4.17	4.10	9.41	0.99	0.88
Bi	201.0	167.9	54.3	9.80	2.04	25.07	2.52	11.33	2.72	0.10	0.11	0.46	1.45	2.92	6.16	2.01	0.71
BCr	178.5	164.1	57.0	9.80	1.85	27.18	3.17	11.19	3.08	0.12	0.13	0.48	5.43	1.64	4.73	0.30	1.50

Fed = Fe extracted by dithionite-citrate-bicarbonate (DCB), method described in Mehra and Jackson (1960) with modifications of Inda Junior and Kämpf (2003); Feo = Fe extracted by acid ammonium oxalate (AAO) (Schwertmann, 1964); Ald = Al extracted by DCB (Mehra and Jackson, 1960); Alo = Al extracted by AAO (Schwertmann, 1964); Ki = 1.7 × SiO_2/Al_2O_3 (Vettori, 1969); Fed/Fes = Fe extracted by DCB/Fe extracted by sulfuric digestion (Vettori, 1969); nd = not determined. C-HA/C-FA = ratio between carbon content in the form of humic acids (C-HA) and fulvic acids (C-FA); C-AE/C-HUM = ratio of the alkaline extract carbon content (sum of C-FA and C-HA) and the humin fraction carbon content (C-HUM), all determined according to Mendonça and Matos (2005).

The FA fractions have the lowest contents of C (C-FA). The C-FA contents in the anthropogenic horizons range from 2.17 to 4.17 g kg^{-1} in the ADE profiles and from 4.26 to 7.24 g kg^{-1} in the ME profiles, decreasing in the subsurface for all the profiles, as indicated by the high HAF/FAF ratios (Table 4).

Archaeological Dark Earth has the highest C-HA/C-FA ratios relative to the ME profiles, with high values in the anthropogenic horizons of 5.64 in the P1 Au2 horizon and 6.67 in the P2 Au horizon (Table 4), indicating predominance of the HA fraction over FA.

The ADE profiles have C-AE/C-HUM ratio values of less than 1 for all horizons, except for the P2 Au horizon, which has a value of 1.10. In most of these soils, the values are less than 0.5, with the lowest values at depth, thus indicating higher humic fraction stability in these soils. The P3 and P4 profiles have higher C-AE/C-HUM ratio values, which are greater than 1 for P3, except for the Aup and BCr horizons. Fontana et al. (2010), studying organic matter fractionation and the characterization of humic acids, determined C-AE/C-HUM ratio values between 0.2 and 7.2.

The HUM contents are primarily correlated with the Ca values ($r = 0.86$, $p<0.001$), Mg ($r = 0.68$, $p<0.001$), and the poorly formed crystalline structures of Al and Fe (Alo: $r = 0.72$, $p<0.001$; Feo: $r = 0.45$, $p<0.10$). The HA and TOC have behavior similar to HUM, highlighting the close relationship ($p<0.001$) with Alo ($r = 0.92$ and $r = 0.87$, respectively). The FA is inversely related to Fed ($p<0.01$) and Ald ($p<0.10$) (Table 5).

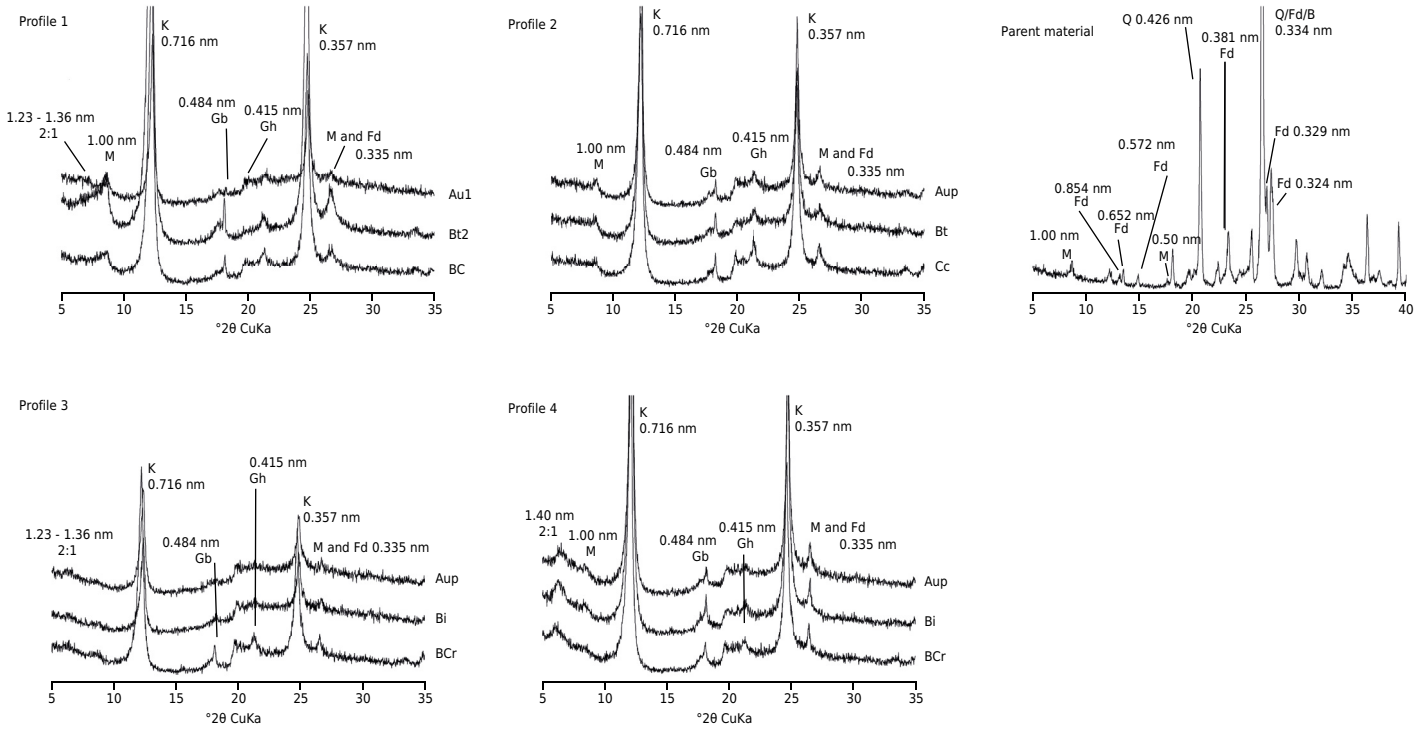

Figure 3. X-ray diffraction (XRD) of the natural clay fraction in the form of oriented aggregates from the A, B, and C horizons/layers and of the parent material. Kaolinite (K), gibbsite (Gb), goethite (Gh), mica (M), feldspars (Fd), smectite (S), vermiculite (V), biotite (B), and quartz (Q).

Table 5. Coefficient of determination (r) between fractions of the soil organic matter and soil parameters of Archaeological Dark Earth and Mulatto Earth in western Amazonia, Brazil

SOM fractions	Ca^{+2}	Mg^{+2}	Fed	Feo	Ald	Alo
			r			
TOC	0.86^{***}	0.73^{***}	-0.08^{ns}	0.57^{**}	0.24^{ns}	0.87^{***}
C-HUM	0.86^{***}	0.68^{***}	-0.12^{ns}	0.45^{*}	0.14^{ns}	0.72^{***}
C-HA	0.68^{***}	0.60^{**}	-0.21^{ns}	0.55^{*}	0.11^{ns}	0.92^{***}
C-FA	0.13^{ns}	-0.02^{ns}	-0.59^{**}	0.28^{ns}	-0.54^{*}	0.37^{ns}

Values shown are significant at the level of $p<0.001$ (***), $p<0.01$ (**), and $p<0.10$ (*); ns = no significant difference.

Thus, meeting the requirements of the SiBCS (Santos, 2013b) and WRB (IUSS Working Group WRB, 2015), the soil class distributions from the summit to the footslope follow the sequence: P1 - *Luvissolo Crômico Órtico típico* (Humic, Pretic Luvisol); P2 - *Luvissolo Crômico Pálico típico* (Humic, Pretic Luvisol); and P3 and P4 - *Cambissolo Háplico Ta Distrófico típico* (Clayic, Dystric).

DISCUSSION

Pedogenesis and pre-Colombian land use indicate significant differences in the soil profiles studied along the toposequence in southern Amazonia. The soil properties suggest that pedogenesis in all pedons are associated with organic matter accumulation, such as melanization, humification, and formation of organometallic complexes, as indicated by high levels of organic carbon combined with the dark-colored uppermost horizons (values and chromas ≤3 wet), P, and carbon-oxides. Melanization of the anthropic horizons is related to the higher quantity of charcoal micro-particles (Macedo et al., 2017) as a result of anthrosolization. The anthropic horizons of studied ADE and ME are morphologically different, probably indicating different levels of melanization. Archaeological Dark Earth

have black to very dark brown material and are thicker, while very dark grayish brown horizons are predominant in the ME (except Aup of P3) as a consequence of the higher quantities of organic carbon and ceramic artifacts in ADE, suggesting more intense anthropogenesis that probably contributed to melanization.

The higher fertility of ADE compared to ME indicates the diversification of the pre-Columbian anthropic activity, also supported by the quantity of ceramic artifacts, which is significantly higher in the ADE (Fraser et al., 2011). The abrupt change in the values of the FS/CS ratio between the Aup and AB horizons of P4 suggests that the anthropic horizon are deposited. Change in this ratio is less pronounced in P3 (Table 2). Both P3 and P4 are ME. Some authors have suggested that the A horizon of ME was deposited after being removed from organic surface horizons or river materials by cutting tools (Arroyo-Kalin et al., 2009; Denevan, 2009); however, in the present study, there is little evidence that demonstrates such deposition. Macedo et al. (2017) showed that these coatings in the B horizon below the pretic horizon are argilluviation features degraded by bioturbation, unrelated to the deposition of material.

The high fertility of the non-anthropic subsurface horizons, validated by the high base saturation (V) and the high levels of P and organic carbon, shows that the anthropic impact is not limited to the surface horizons (Aup and Au), but can modify the soil at depth via pedogenic processes such as melanization and bioturbation (Kern and Kämpf, 2005). These values are greater than in non-anthropogenic soils observed by Campos et al. (2012), who found that the values of pH, organic carbon, and total bases were higher in the archaeological dark earths in the Manicoré region, southern Amazon. This high fertility in the subsurface horizons is more evident in the ADE, but the P3 and P4 profiles (ME) have high levels of Ca^{2+} and organic carbon in the subsurface horizons. It is unlikely that any well-drained Tertiary Plateau environment could contain high contents of P, Ca^{2+}, and Mg^{2+}, such as those reported here, without anthropic influence. Bioturbation is considered a crucial process of melanization for the A horizons with Bt, as indicated by earthworm channels filled with material in the Bt horizons and with Bt horizon material occurring in the A horizons, as observed by Lima et al. (2002). Translocation of charcoal to subsurface horizons was identified in a study conducted by Macedo et al. (2017), transforming transitional and subsurface horizons into anthropic horizons.

The high values determined for Ca^{2+} in these pedons likely originate from the deposition of human and animal bones (Lima et al., 2002). Recent studies show that less human action on ME is required to generate lower levels of nutrients, such as Ca^{2+} and Mg^{2+}, compared to ADE (Fraser et al., 2011). Lower contents of K^{+} were also observed by Santos et al. (2013a) and Barros et al. (2012), who determined similar K^{+} values in anthropic soils of the Amazon. These CEC and V values are usually found in Amazonian anthropic soils (Glaser and Birk, 2012).

The low Al saturation in the ADE is a result of pH values greater than 5.4. The high potential acidity and low levels of Al^{3+} in all profiles indicate that the acidity is primarily composed of H ions, which may be associated with addition of H^{+} via SOM decomposition (Barbosa Filho et al., 2005).

Bulk densities are lowest in the upper horizons due to larger pore spaces created from organic matter input, as indicated by the Pt values (Table 2), and increases within the subsurface horizons due to plugging from illuviated clays and greater contents of Fed. The DF of clay increases at the surface due to the influence of higher organic matter contents (Prado and Centurion 2001; Sombroek et al., 2009).

High P values (Table 3) may be due to the large accumulation of bonfire ash, tortoise shells, fish, and other animal bones (Smith, 1980; Glaser and Birk, 2012), which may also be associated with microfragments of bony apatite with high P/Ca values (Lima et al., 2002). The P2 profile (ADE) may have received a higher deposition of residues, as indicated by

the high values of P. In addition, there was a greater tendency of accumulation at the convex inflection (shoulder) and hillside areas of the anthropic soils. This indicated a preference for plant and animal waste disposal within the outskirts of the pre-Columbian settlements (Kern and Kämpf, 2005).

The TOC and OM(NaOH) content and compositional differences between ADE and ME are likely due to the anthropogenic origin of these soils, which were irregular deposits with the presence of carbonized material (Madari et al., 2009) and/or exhibited different human occupational phases over time and different soil usages (Glaser and Birk, 2012). All the soil profiles are dominated by strongly humified fractions, with smaller amounts of more soluble and mobile FA fractions, as indicated by the C-HA/C-FA ratios. The C-HA/C-FA values higher than 1.0 indicate predominance of the HA fraction over FA, which is an indicator of humus quality. The predominance of the most stable fractions (humin and humic acids) is also verified by Lima et al. (2002).

However, the difference observed in this ratio, significantly lower for the ME profiles than for the ADE profiles, indicates that the soil organic matter stability mechanisms may be different between ADE and ME, which should be considered for soil use and management to reduce C losses. This difference may be related to the organic matter origin. The ADE seems to have been developed from household refuse of pre-Columbian villages (ashes and cooking coals), garden and crop residues, feces, and bones. The ME may be related to intentional application of human or animal waste, green manure from forest or river materials, charcoal and ash, and fishing and hunting residues, which would allow for intensive or semi-intensive farming (Denevan, 2009).

The low C-AE/C-HUM ratio values (≤ 0.5) are indicative of strong organic matter stability and/or its interaction with the mineral fraction and can, therefore, be evaluated as an indicator of soil organic matter stability (Fontana et al., 2010). The lower C-AE/C-HUM ratio values in the ADE suggest that formation of the organomineral complex is a very important mechanism of organic matter stability in the P1 and P2 profiles (ADE). The HUM fraction has a significantly larger contribution from black carbon related pyrolysis products compared to the HA and FA fractions (Schellekens et al., 2017). This suggests the presence of condensed aromatic structures (not extractable with NaOH) and/or that the organomineral interaction may be significant for the soils studied because NaOH does not extract the strong mineral-bound structures (Knicker et al., 2005).

Our results show that the organometallic complexes are formed primarily by association between the more humified organic fractions and the Ca^{2+}, Mg^{2+}, and oxalate extracted Al forms, as indicated by their close relationships ($p<0.001$). The Feo ($p<0.10$) also contributes to carbon stability in the soils studied (Table 5).

The soil profiles reported here developed on volcanic rocks (andesites/rhyodacites), unlike most of the ADE described in the state of Amazonas, which developed on unconsolidated sediments. This difference in parent material may be the primary cause of the high-activity clays in these soils (ADE and ME) (Table 3), even in the Amazonian environment.

The mica expressions verified in the clay fraction diffractograms (Figure 3) of the soils along the toposequence may be inherited from the parent material of these soils. This is supported by the parent material XRD diffractograms of the P1 (ADE) and P3 (ME) profiles, which indicate the occurrence of biotite (Figure 3). The occurrence of expansive minerals in the soil is likely the result of mica alteration. Previous studies indicate that 2:1 minerals (expansive) are not found in upslope Tertiary Plateau soils (Lima et al., 2002). Thus, the soils studied are distinguished from Amazonian anthropic soils and the vast majority of other soils (Tertiary Plateau, called *Terra Firme* in the region) in the Amazon region.

The occurrence of ADE on Luvisol is unprecedented in the Amazon region. However, our results show that the ADE studied are on the Luvisols, which may have contributed to create the ADE. The origin of ADE is still controversial among researchers; however, the

widely accepted hypothesis is that these soils are unintentionally formed by pre-Columbian anthropogenic activity (Woods and Mccann, 2001). Since most Luvisols are fertile soils and suitable for a wide range of agricultural uses (IUSS Working Group WRB, 2015), the land use by ancient Amazonian humans and the formation of anthropogenic soils on Luvisols suggests they did not attempt to improve soil fertility.

In areas of similar parent material and climate, formation of the Bt horizons may be dependent on anthropogenic activities (Macedo et al., 2017). The weathering and clay formation, besides the clay eluviation, are insufficient for textural horizon characterization. The Bt2 and Bt horizons of the P1 and P2, respectively, are identified by means of clay coatings. Anthropic activities can favor argilluviation according to Macedo et al. (2017), who found that clay coatings on the ceramic fragments and in the pores demonstrate, surprisingly, that this is a current process. In the present study, argilluviation may be favored by higher humic acid values in ADE (Table 4), which increases the electronegativity of these soils due to the higher total acidity of humic acids, with a higher O/H ratio of this humic fraction in pretic horizons (Madari et al., 2009).

In contrast, the ME has no clay coatings, which suggests that intensive land use must have promoted stress in the particles and local reorganization of clay minerals and/or poor argilluviation, or no argilluviation, since it is a soil with a low degree of formation. Therefore, the understanding of this soil formation is limited without considering anthropogenic activity (Lehmann et al., 2003; Sandor et al., 2005; Arroyo-Kalin et al., 2009; Arroyo-Kalin, 2012; Macedo et al., 2017).

The silt/clay ratio is used as an auxiliary index to indicate the degree of soil weathering; thus, the higher the value of this ratio, the smaller the degree of weathering (Jacomine, 2005). The silt/clay ratio in the profiles studied has higher values in the anthropic horizons. A higher silt/clay ratio in the anthropic horizon was observed by Aquino et al. (2016) and Sombroek et al. (2009), these latter indicate that this relationship is due to inefficient dispersion of the clay particles and/or fusion of particles that result in an increase in the silt fraction. Our results also show that the first few centimeters of the upper soil layer became sandier (Smith, 1980; Sombroek et al., 2009). The exposed soil is more susceptible to erosion, which causes removal of clay and silt particles, or even clay migration to the subsurface horizons.

Furthermore, the Ki values of ADFE indicate a lower degree of soil weathering in the footslope soils (P4, Table 4). The higher Ki values are attributed to higher Si contents in the parent material, the Si is derived from feldspars present in the soil parent material (Figure 3). This is one of the factors that explains the higher Si and Al levels in the system, validated by the SiO_2 and Al_2O_3 values of sulfur digestion. For the P4 profile, the moderate degree of drainage leads to higher values of Si and Ki, as observed by Ghidin et al. (2006). The Ki index also implies a kaolinitic mineralogy, which was validated via DRX (Figure 3).

The low Fe_2O_3 values are due to a relative lack of Fe in the parent material (intermediate volcanic rocks). These results agree with the results of studies on Amazon soils by Silva et al. (2011). Higher values of Feo from anthropic A horizons were also found by Lima et al. (2002). This is consistent with the distribution of organic C in these profiles. Soil organic matter is a significant inhibitor of Fe oxide crystallization (Naramabuye and Haynes, 2006). The small variation of TiO_2 within each profile shows the uniformity of the source materials studied, disproving a possible lithological discontinuity (Mafra et al., 2001). The similarity of ρs along the entire toposequence also indicates homogeneity of the material among the areas (Sombroek et al., 2009).

CONCLUSIONS

Anthropic soils along a toposequence in western Amazonia, Brazil, are classified as Pretic Luvisols (Archaeological Dark Earth, ADE) and Dystric Cambisols (Mulatto Earth,

ME). The soil forming processes in all the profiles are associated with organic matter accumulation, such as humification and melanization. The occurrence of ADE on Luvisol has not previously been described in the Amazon region.

Occupation of long-term pre-Columbian human inhabitants in the study area increased the thickness of the anthropic A horizons and caused them to be eutrophic and high in organic carbon content and available P in ADE relative to ME. The occurrence of high-activity clays (traces of expansive minerals) in all the profiles is derived from the parent volcanic material, distinguishing the soils studied from other Amazonian soils and from other anthropogenic soils of *Terra Firme*.

Humidified carbon accumulation (extracted with NaOH) in the ADE and ME soils suggests differences in the composition and mechanisms of soil organic matter stability. In all anthropic soils, forms of aluminum (extracted with ammonium oxalate) and exchangeable Ca and Mg are the primary influence on accumulation of total organic carbon and humin and humic acid fractions. Poorly crystalline iron are also linked with organic fractions, except for fulvic acid.

ACKNOWLEDGMENTS

We thank the *Fundação de Amparo à Pesquisa do Estado do Amazonas* (FAPEAM), the *Secretaria de Estado de Ciência, Tecnologia e Inovação* (SECTI-AM) for granting a scholarship through the *Programa RH – Interiorização* (public notice No. 027/ 2011). We also thank the Professor Mateus Rosas Ribeiro for important contributions to this research, and Embrapa Acre for support during samplings of soil profiles.

REFERENCES

Anjos LHC, Pereira MG, Fontana A. Matéria orgânica e pedogênese. In: Santos GA, Silva LS, Canellas LP, Camargo FAO, editores. Fundamentos da matéria orgânica do solo: ecossistemas tropicais e subtropicais. 2. ed. rev. atual ampl. Porto Alegre: Metrópole; 2008. p. 65-86.

Aquino RE, Marques Junior J, Campos MCC, Oliveira IA, Bahia ASRS, Santos LAC. Characteristics of color and iron oxides of clay fraction in Archeological Dark Earth in Apuí region, southern Amazonas. Geoderma. 2016;262:35-44. https://doi.org/10.1016/j.geoderma.2015.07.010

Arroyo-Kalin M. Slash-burn-and-churn: landscape history and crop cultivation in pre-Columbian Amazonia. Quatern Int. 2012;249:4-18. https://doi.org/10.1016/j.quaint.2011.08.004

Arroyo-Kalin M, Neves EG, Woods WI. Anthropogenic Dark Earth of the Central Amazon region: remarks on their evolution and polygenetic composition. In: Woods WI, Teixeira WG, Lehmann J, Steiner C, WinklerPrins AMGA, Rebellato L, editors. Amazonian dark earth: Wim Sombroek's vision. Berlin: Springer; 2009. p. 99-125.

Barbosa Filho MP, Fageria NK, Zimmermann FJP. Atributos de fertilidade do solo e produtividade do feijoeiro e da soja influenciados pela calagem em superfície e incorporada. Cienc Agrotec. 2005;29:507-14. https://doi.org/10.1590/S1413-70542005000300001

Barros KRM, Lima HV, Canellas LP, Kern DC. Fracionamento químico da matéria orgânica e caracterização física de Terra Preta de Índio. Rev Cien Agrar. 2012;55:44-51. https://doi.org/10.4322/rca.2012.037

Benites VM, Madari B, Machado PLOA. Extração e fracionamento quantitativo de substâncias húmicas do solo: um procedimento simplificado de baixo custo. Rio de Janeiro: Embrapa Solos; 2003. (Comunicado Técnico, 16).

Brasil. Ministério das Minas e Energia. Projeto Radambrasil. Folha SD. 20 Purus: geologia, geomorfologia, pedologia, vegetação, uso potencial da terra. Rio de Janeiro: Departamento Nacional da Produção Mineral; 1978. (Levantamento de Recursos Naturais, 17).

Brasil. Ministério das Minas e Energia. Projeto Radambrasil. Folha SD. 2l Tapajós: geologia, geomorfologia, solos, vegetação e uso potencial da terra. Rio de Janeiro: Departamento Nacional da Produção Mineral; 1975. (Levantamento de Recursos Naturais, 7).

Brown G, Brindley GW. X-ray diffraction procedures for clay mineral identification. In: Brindley GW, Brown G, editors. Crystal structures of clay minerals and their X-ray identification. London: Mineralogical Society; 1980. p. 305-60.

Bryant RB, Galbraith JM. Incorporating anthropogenic processes in soil classification. In: Eswaran H, Rice T, Ahrens R, Stewart BA, editors. Soil classification: a global desk reference. Boca Raton: CRC Press; 2003. p. 57-66.

Campos MCC, Ribeiro MR, Souza Júnior VS, Ribeiro Filho MR, Souza RVCC, Almeida MC. Caracterização e classificação de terras pretas arqueológicas na Região do Médio Rio Madeira. Bragantia. 2011;70:598-609. https://doi.org/10.1590/S0006-87052011000300016

Campos MCC, Santos LAC, Silva DMP, Mantovanelli BC, Soares MDR. Caracterização física e química de terras pretas arqueológicas e de solos não antropogênicos na região de Manicoré, Amazonas. Revista Agro@mbiente On-line. 2012;6:102-9. https://doi.org/10.18227/1982-8470ragro.v6i2.682

Costa JA, Costa ML, Kern DC. Analysis of the spatial distribution of geochemical signatures for the identification of prehistoric settlement patterns in ADE and TMA sites in the lower Amazon Basin. J Archaeol Sci. 2013;40:2771-82. https://doi.org/10.1016/j.jas.2012.12.027

Costa ML, Kern DC. Geochemical signatures of tropical soils with archaeological black earth in the Amazon, Brazil. J Geochem Explor. 1999;66:369-85. https://doi.org/10.1016/S0375-6742(99)00038-2

Cunha P, Marques Júnior J, Curi N, Pereira GT, Lepsch IF. Superfícies geomórficas e atributos de Latossolos em uma sequência arenítico-basáltica da região de Jaboticabal (SP). Rev Bras Cienc Solo. 2005;29:81-90. https://doi.org/10.1590/S0100-06832005000100009

Dalrymple JB, Blong RJ, Conacher AJ. A hipothetical nine unit land a surface model. Z Geomorphol. 1968;12:60-76.

Denevan W. As origens agrícolas da Terra Mulata na Amazônia. In: Teixeira WG, Kern DC, Madari BE, Lima HN, Woods W, editores. As Terras Pretas de Índio da Amazônia: sua caracterização e uso deste conhecimento na criação de novas áreas. Manaus: Embrapa Amazônia Ocidental; 2009. p. 82-6.

Donagema GK, Campos DVB, Calderano SB, Teixeira WG, Viana JHM. Manual de métodos de análise do solo. 2. ed. rev. Rio de Janeiro: Embrapa Solos; 2011.

Flint AL, Flint LE. Particle density. In: Dane JH, Topp CG, editors. Methods of soil analysis: physical methods. 3rd ed. Madison: Soil Science Society of America; 2002. Pt. 4. p. 229-40.

Fontana A, Pereira MG, Anjos LHC, Benites VM. Quantificação e utilização das frações húmicas como característica diferencial em horizontes diagnósticos de solos brasileiros. Rev Bras Cienc Solo. 2010;34:1241-57. https://doi.org/10.1590/S0100-06832010000400023

Fraser J, Teixeira W, Falcão N, Woods W, Lehmann J, Junqueira AB. Anthropogenic soils in the Central Amazon: from categories to a continuum. Area. 2011;43:264-73. https://doi.org/10.1111/j.1475-4762.2011.00999.x

Gee GW, Or D. Particle-size analysis. In: Dane JH, Topp CG, editors. Methods of soil analysis: physical methods. 3rd ed. Madison: Soil Science Society of America; 2002. Pt. 4. p. 255-93.

Ghidin AA, Melo VF, Lima VC, Lima JMJC. Topossequência de Latossolos originados de rochas basálticas no Paraná. I - mineralogia da fração argila. Rev Bras Cienc Solo. 2006;30:293-306. https://doi.org/10.1590/S0100-06832006000200010

Glaser B, Birk JJ. State of the scientific knowledge on properties and genesis of Anthropogenic Dark Earths in Central Amazonia (*Terra Preta de Índio*). Geochim Cosmochim Ac. 2012;82:39-51. https://doi.org/10.1016/j.gca.2010.11.029

Glaser B, Guggenberger G, Zech W, Ruivo ML. Soil organic matter stability in Amazon dark earths. In: Lehmann J, Kern DC, Glaser B, Woods WI, editor. Amazonian dark earths: origin, properties, management. Dordrecht: Kluwer Academic Publishers; 2003. p. 141-58.

Grossman RB, Reinsch TG. Bulk density and linear extensibility. In: Dane JH, Topp CG, editors. Methods of soil analysis: physical methods. 3rd ed. Madison: Soil Science Society of America; 2002. Pt. 4. p. 201-28.

Inda Junior AV, Kämpf N. Avaliação de procedimentos de extração dos óxidos de ferro pedogênicos com ditionito-citrato-bicarbonato de sódio. Rev Bras Cienc Solo. 2003;27:1139-47. https://doi.org/10.1590/S0100-06832003000600018

IUSS Working Group WRB. World reference base for soil resources 2014, update 2015: International soil classification system for naming soils and creating legends for soil maps. Rome: Food and Agriculture Organization of the United Nations; 2015. (World Soil Resources Reports, 106).

Jackson ML. Soil chemical analysis advanced course. 2nd ed. Madison: University of Wisconsin; 1975.

Jacomine PKT. Origem e evolução dos conceitos e definições de atributos, horizontes diagnósticos e das classes de solos do Sistema Brasileiro de Classificação de Solos (SiBCS). In: Vidal-Torrado P, Alleoni LRF, Cooper M, Silva AP, Cardoso EJ, editores. Tópicos em ciência do solo. Viçosa, MG: Sociedade Brasileira de Ciência do Solo; 2005. v. 4. p. 193-231.

Kern DC, D'Aquino G, Rodrigues TE, Frazão FJL, Sombroek W, Neves EG, Myers TP, Neves EG. Distribution of antropogenic dark earths. In: Lehmann J, Kern DC, Glaser B, Woods WI, editors. Amazonian dark earths: origin, properties, management. Dordrecht: Kluwer Academic Publishers; 2003. p. 51-76.

Kern DC, Kämpf N. Ação antrópica e pedogênese em solos com Terra Preta em Cachoeira-Porteira, Pará. Bol Mus Para Emílio Goeldi. 2005;1:187-201.

Kern DC, Kämpf N. Antigos assentamentos indígenas na formação de solos com Terra Preta Arqueológica na região de Oriximiná, Pará. Rev Bras Cienc Solo. 1989;13:219-25.

Knicker H, González-Vila FJ, Polvillo O, González JA, Almendros G. Fire-induced transformation of C- and N- forms in different organic soil fractions from a Dystric Cambisol under a Mediterranean pine forest (*Pinus pinaster*). Soil Biol Biochem. 2005;37:701-18. https://doi.org/10.1016/j.soilbio.2004.09.008

Lehmann J, Kern DC, German LA, Mccann J, Martins GC, Moreira A. Soil fertility and production potential. In: Lehmann J, Kern DC, Glaser B, Woods WI, editors. Amazonian dark earths: origin, properties, management. Dordrecht: Kluwer Academic Publishers; 2003. p. 105-24.

Lichtfouse E, Leblond C, Silva M, Behar F. Occurrence of biomarkers and straight-chain biopolymers in humin: implication for the origin of soil organic matter. Naturwissenschaften. 1998;85:497-501. https://doi.org/10.1007/s001140050538

Lima HN, Schaefer CER, Mello JWV, Gilkes RJ, Ker JC. Pedogenesis and pre-Columbian land use of "Terra Preta Anthrosols" ("Indian black earth") of Western Amazonia. Geoderma. 2002;110:1-17. https://doi.org/10.1016/S0016-7061(02)00141-6

Macedo RS, Teixeira WG, Corrêa MM, Martins GC, Vidal-Torrado P. Pedogenetic processes in Anthrosols with pretic horizon (Amazonian Dark Earth) in Central Amazon, Brazil. PloS ONE. 2017;12:e0178038. https://doi.org/10.1371/journal.pone.0178038

Madari BE, Cunha TJF, Novotny EH, Milori DMBP, Martin Neto L, Benites VM, Coelho MR, Santos GA. Matéria orgânica dos solos antrópicos da Amazônia (Terra Preta de Índio): suas características e papel na sustentabilidade da fertilidade do solo. In: Teixeira WG, Kern DC, Madari BE, Lima HN, Woods W, editores. As Terras Pretas de Índio da Amazônia: sua caracterização e uso deste conhecimento na criação de novas áreas. Manaus: Embrapa Amazônia Ocidental; 2009. p. 172-89.

Mafra AL, Silva EF, Cooper M, Demattê JLI. Pedogênese de uma sequência de solos desenvolvidos de arenito na região de Piracicaba (SP). Rev Bras Cienc Solo. 2001;25:355-69. https://doi.org/10.1590/S0100-06832001000200012

Mehra OP, Jackson ML. Iron oxide removal from soils and clays by a dithionite-citrate system buffered with sodium bicarbonate. Clay Clay Miner. 1960;7:317-27. https://doi.org/10.1346/CCMN.1958.0070122

Mendonça ES, Matos ES. Matéria orgânica do solo: métodos de análises. Viçosa, MG: Universidade Federal de Viçosa; 2005.

Naramabuye FX, Haynes RJ. Short-term effects of three animal manures on soil pH and Al solubility. Aust J Soil Res. 2006;44:515-21. https://doi.org/10.1071/SR05062

Prado RM, Centurion JF. Alterações na cor e no grau de floculação de um Latossolo Vermelho-Escuro sob cultivo contínuo de cana-de-açúcar. Pesq Agropec Bras. 2001;36:197-203. https://doi.org/10.1590/S0100-204X2001000100024

Roberts P, Hunt C, Arroyo-Kalin M, Evans D, Boivin N. The deep human prehistory of global tropical forests and its relevance for modern conservation. Nat Plants. 2017;3:17093. https://doi.org/10.1038/nplants.2017.93

Sandor J, Burras CL, Thompson M. Factors of soil formation: human impacts. In: Hillel D, editor. Encyclopedia of soils in the environment. New York: Academic Press; 2005. p. 520-32.

Santos HG, Jacomine PKT, Anjos LHC, Oliveira VA, Oliveira JB, Coelho MR, Lumbreras JF, Cunha TJF. Sistema brasileiro de classificação de solos. 3. ed. rev. ampl. Rio de Janeiro: Embrapa Solos; 2013b.

Santos LAC, Campos MCC, Aquino RE, Bergamin AC, Silva DMP, Marques Junior J, França ABC. Caracterização de terras pretas arqueológicas no sul do estado do Amazonas. Rev Bras Cienc Solo. 2013a;37:825-36. http://dx.doi.org/10.1590/S0100-06832013000400001

Santos RD, Lemos RC, Santos HG, Ker JC, Anjos LHC, Shimizu SH. Manual de descrição e coleta de solo no campo. 7. ed. rev. ampl. Viçosa, MG: Sociedade Brasileira de Ciência do Solo; 2015.

Schellekens J, Almeida-Santos T, Macedo RS, Buurman P, Kuyper TW, Vidal-Torrado P. Molecular composition of several soil organic matter fractions from anthropogenic black soils (Terra Preta de Índio) in Amazonia - a pyrolysis-GC/MS study. Geoderma. 2017;288:154-65. https://doi.org/10.1016/j.geoderma.2016.11.001

Schwertmann U. Differenzierung der eisenoxide des bodens durch extraktion mit ammoniumoxalat-lösung. J Plant Nutr Soil Sc. 1964;105:194-202. https://doi.org/10.1002/jpln.3591050303

Serviço Geológico do Brasil - CPRM. Base cartográfica digital obtida pela CPRM, a partir da base cartográfica integrada digital do Brasil ao milionésimo elaborada pelo IBGE. Manaus: Sureg; 2005.

Silva FWR, Lima HN, Teixeira WG, Motta MB, Santana RM. Caracterização química e mineralogia de solos antrópicos (Terras Pretas de Índio) na Amazônia Central. Rev Bras Cienc Solo. 2011;35:673-81. https://doi.org/10.1590/S0100-06832011000300002

Smith NJH. Anthrosols and human carrying capacity in Amazonia. Ann Assoc Am Geogr. 1980;70:553-66. https://doi.org/10.1111/j.1467-8306.1980.tb01332.x

Sollins P, Homann P, Caldwell BA. Stabilization and destabilization of soil organic matter: mechanisms and controls. Geoderma. 1996;74:65-105. https://doi.org/10.1016/S0016-7061(96)00036-5

Sombroek W. Amazon soil: a reconnaissance of the soils of the Brazilian Amazon Region. Wageningen: Centre for Agricultural Publications and Documentation; 1966.

Sombroek W, Kern D, Rodrigues T, Cravo MS, Cunha TJF, Woods W, Glaser B. Terra Preta e Terra Mulata: suas potencialidades agrícolas, suas sustentabilidades e suas reproduções. In: Teixeira WG, Kern DC, Madari BE, Lima HN, Woods W, editores. As Terras Pretas de Índio da Amazônia: sua caracterização e uso deste conhecimento na criação de novas áreas. Manaus: Embrapa Amazônia Ocidental; 2009. p. 251-7.

Statsoft Inc. Statistica - Data analysis software system. 12th ed. Austrália: Statsoft Software; 2013.

Swift RS. Organic matter characterization. In: Sparks DL, Page AL, Helmke PA, Loeppert RH, editors. Methods of soil analysis: chemical methods. Madison: Soil Science Society of America; 1996. Pt. 3. p. 1011-69.

Vettori L. Métodos de análise de solo. Rio de Janeiro: Equipe de Pedologia e Fertilidade do Solo; 1969. (Boletim Técnico, 7).

Woods WI, McCann JM. El origen y persistencia de las tierras negras de la Amazonía. In: Hiraoka M, Mora S, editors. Desarrollo sostentible en la Amazonía: mito o realidad? Quito: Abya-Yala; 2001. p. 23-30.

Yeomans JC, Bremner JM. A rapid and precise method for routine determination of organic carbon in soil. Commun Soil Sci Plan. 1988;19:1467-76. https://doi.org/10.1080/00103628809368027